Hindawi
Mathematical Problems in Engineering
Volume 2019, Article ID 2747205, 13 pages
https://doi.org/10.1155/2019/2747205

Research Article

Analysis of Vertical Vibration Mechanism of Reciprocating Compressors considering Flexibility of Piston Rod and Crosshead Subsidence

Shouguo Cheng,[1,2] Shulin Liu ,[1] Shungen Xiao ,[1,3] Dong Li,[4] and Xin Sun[1]

[1]*School of Mechatronics Engineering and Automation, Shanghai University, Shanghai, China*
[2]*Department of Mechanical and Electrical Engineering, Jiangyin Polytechnic College, Jiangyin, China*
[3]*College of Information, Mechanical and Electrical Engineering, Ningde Normal University, Ningde, China*
[4]*School of Petroleum Engineering, Changzhou University, Changzhou, China*

Correspondence should be addressed to Shulin Liu; lsl346@126.com and Shungen Xiao; xiaoshungen022@163.com

Received 2 September 2018; Revised 13 January 2019; Accepted 14 January 2019; Published 20 February 2019

Academic Editor: Roman Lewandowski

This paper is targeted on the vertical vibration of the crosshead in a reciprocating compressor, taking into consideration the crosshead subsidence. The traditional model of the compressor is usually a crank-slider mechanism system without considering the abrasion loss for any parts, thus neglecting the influence of the piston rod flexibility. A rigid-flexible model of slider-crank is described theoretically, in which the crank, connecting rod, and crosshead are treated as rigid bodies, while the piston rod connected to the crosshead is considered as a flexible body. Lagrange equation was adopted to establish the kinetic equation of the system, considering the mass of the crank, the linkage, and the crosshead. After modeling the mechanism, the simulation shows that the dynamic response of the crosshead will be greatly influenced if crosshead subsidence is considered. Additionally, the influence of the crosshead subsidence is also investigated, and some new phenomena arise especially the vertical vibration of crosshead.

1. Introduction

A reciprocating compressor is one of the most widely used machines in petroleum and chemical production processes, such as gas compression and natural gas transportation [1]. Failures of crosshead and other moving parts of reciprocating compressor are not only unpredictable but also very harmful. So far, there has been no efficient solution revealing the failures based on vibration signal of shell due to the lack of transferring mechanism of fault information. In the past several decades, fault diagnose technologies did not make much progress in terms of reciprocating compressors because of so many excitation sources. The reasons can be attributed to three aspects. First of all, in each working period of reciprocating compressors, the working load of the air cylinder changes with time goes by and so do some key parts of the reciprocating compressors. As a result, causes of the fault are often complicated due to the complexity of signals. Meanwhile, the behavior of kinetics and some fault information are highly nonlinear, leading to the fact that theories suitable for rotating machines are not appropriate for reciprocating compressors [2]. Secondly, the key parts of reciprocating compressors are inside the body, which is difficult to approach and test. Simultaneously, how the vibration signals transfer in the whole process is still uncertain, although there are already some conclusions about the transferring routes. As a consequence, extractions of fault signals are sometimes aimless and blind. Finally, there are so many origins of vibrations in the system of reciprocating compressor, which is the reason why the extractions of proposed signal are often a difficult task and lack precision.

To conclude, if fault diagnose methods for reciprocating compressors can be based on the analysis of dynamic model which contains a kind of specific fault signals, the process of diagnosing fault signals will be more efficient. Many researches on the dynamic analysis of reciprocating compressors have been done by many researchers. Volkan Parlaktaş and Engin Tanik [3] introduced a single piece

spatial compliant slider-crank mechanism. In his model, deflections of the multiple axis flexural hinges are determined as bending and twist separately. Deck J.F. et al. [4] also studied dynamic responses containing clearance in revolute joints. Also Ndiaye and Bernier [5] did a dynamic model of a hermetic reciprocating compressor in on-off cycling operation. Also Farzaneh-Gord et al. [6] optimized design parameters of reciprocating air compressor thermodynamically. They developed a mathematical model according to the mass conservation, first law, and ideal gas assumption to study the performance of reciprocating compressors. R. Singht and W. Soedel [7] built a mathematical model for multicylinder compressors. The technique as outlined in this paper was said to be applicable to any multicylinder positive displacement type of fluid machine. As is known to all, the most common failure in reciprocating compressors is always related to the valves. Recently, Mahmood Farzaneh-Gord and Hossein Khoshnazar [8] have done much study on valve fault detection for single-stage reciprocating compressors, taking into consideration the effect of gas temperature and mass flow rate and in-cylinder pressure and temperature which were usually ignored in many other researches. Additionally, Van Tung Tran and Faisal AlThobiani [9] proposed a scheme for fault diagnosis of reciprocating compressor valves using Teager–Kaiser energy operator and deep belief networks, and this scheme has undoubtedly improved the accuracy of classification of fault signals. Klaus Brun and Sarah Simons [10] have taken into consideration the strong pressure pulsations which are often the cause of instability in a reciprocating compressor. Results provided clear evidence that suction pulsations can significantly reduce the surge margin of a centrifugal compressor.

After about one decade's development, theories of rigid multibody dynamic had made great progress, among which the Euler equation and Lagrange equation are the most important two methods to analyze the multibody dynamics. At the beginning of 1970, many researches began to study the dynamic responses of flexible multibody dynamics, focusing on the modeling of the flexible system and the method to solve the equation. Till now, the research on flexible multibody dynamics is far from perfect although there are already some progresses. In the field of vector mechanics, Newton-Euler method was firstly used because of its clear meaning in physics and its convenience to build an equation. One of the most widely used methods is Lagrange method, which can be applied to both conservative and nonconservative systems. In this article, the Lagrange method is also adopted. Also, in the previous work on reciprocating compressors, much attention was focused on the clearance in the joints, and many models for collision between joints were obtained. And there are a number of publications on the dynamic analysis of slider-crank mechanisms with clearance: Flores et al. have published several papers [11–13] on the dynamics of multibody systems with imperfect joints. Xiaohong Jia et al. [14] have also done investigation on the dynamic performance of the tripod-ball sliding clearance in a crank-slider mechanism.

The rigid-flexible hybrid model of mechanism has been studied by many scholars. S. Yaqubi, M. Dardel, and H. M. Daniali [15] studied nonlinear dynamics and control of crank-slider mechanism with link flexibility and joint clearance. Both the case of the mechanism with rigid link and the case with flexible link were studied through simulation and experimental tests [16]. A.L. Schwab, J.P. Meijaard, and P. Meijers presented the impact model to estimate the maximum contact force during impact [17]. Wang, Zhe et al. [18] presented a modified extended delayed feedback control (EDFC) to stabilize the chaotic motion of the flexible multibody system. M. Dupac and D. G. Beale [19] investigate a planar mechanism with a flexible rod with cracks, in which the cracks are represented by massless rotational springs and link flexibility is modeled by massless rotational springs with the spring constant. Erkaya, S [20] investigate the experimental effects of balancing and link flexibility on the dynamics. S Doğan et al. [21] investigate articulated and compliant spatial mechanisms with clearance joint. Qiang Tian et al. [22] present a new computational methodology for modeling and analysis of planar flexible multibody systems with clearance and lubricated revolute joints based on the absolute nodal coordinate formulation. Selçuk Erkaya and İbrahim Uzmay investigate the suspension effect of the flexible link of a planar four-bar mechanism [23]. Selçuk Erkaya et al. have also joint clearance effects and vibration responses experimentally and theoretically [24, 25]. E. Zheng and X. Zhou [26] investigate the influence of the clearance size, input crank shaft speed, and number of clearance joints on the dynamic response of the mechanism. Xiao et al. [27] investigate the nonlinear dynamical behaviors of the reciprocating compressor with clearance and subsidence of the crosshead, considering the varying cylinder pressure. Xiao et al. [28] investigate the dynamic behavior of a reciprocating compressor system with subsidence fault considering a flexible piston rod.

These researches undoubtedly both contributed a lot to the study of crank-slider mechanism and provided many basic theories on reciprocating compressors for future researches. However, most of the writers did not pay attention to the mechanism about why the vibration actually takes places. Actually, as a key part of reciprocating compressors, the crosshead carries a lot of useful messages, working as a bridge between behaviors of fault and the vibration of the compressor. Most of the studies are dedicated to the mere analysis of the crosshead without considering the load from cylinder. The dynamic responses of crank-slider mechanism are often studied by considering the displacement responses, velocity responses, and acceleration responses.

This paper will fix more attention on the vertical vibration of crosshead, taking into consideration the flexibility of the piston rod and the changing load from the cylinder. The purpose of this paper is to reveal the intrinsic influences of the crosshead when crosshead subsidence is taken into consideration. The dynamic analysis for a model without the crosshead subsidence will be conducted to prove that the crosshead will never jump from the track if the crosshead does not subside in Section 2. A model that considers the crosshead subsidence will be built but ignore some items that are not so important. The reason why this model is built is to give a general idea for readers that if there is crosshead subsidence, the crosshead will undoubtedly jump from its track in Section 3. Based on the previous model, some other

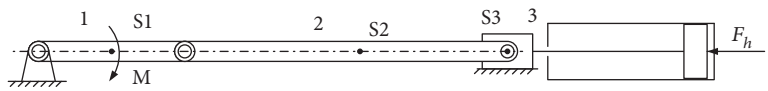

Figure 1: Schematic of the model without the crosshead subsidence.

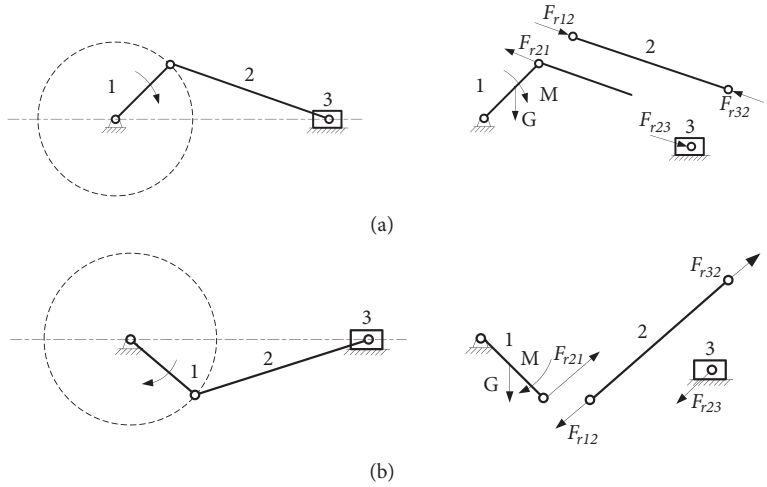

Figure 2: Brief force analysis for a general model without considering crosshead subsidence.

items will be added to the model so that the model will be closer to the real situation. In this model, the Lagrange method is adopted in Section 4. Section 5 summarizes the numerical results and vertical force analysis of reciprocating compressors. In addition, the conclusion of this paper is given in Section 6.

If the rotating speed for the crank is stable, the jumps of crosshead will be varied according to the different value of crosshead subsidence. The order of this paper is according to the working life of reciprocating compressors. That means the value of the crosshead subsidence will be chosen very small as the abrasion is not so serious. As time goes by, the abrasion between crosshead and its track will be more series and some bigger values are chosen to simulate these situations. Actually, the crosshead subsidence should not be big enough in real situations because too much use without replacing some components will not be allowed. However, during the analysis process, some exaggerated assumption and figures are shown in this paper to make ideas more clear.

2. Brief Dynamic Analysis for the Model about the Crosshead Jumps

Figure 1 shows the schematic for reciprocating compressors that does not include the crosshead subsidence, which is also the model commonly discussed in most of researches. The model is simplified to be composed of 4 components: the crank shaft with its center of mass being $S_1(x_1, y_1)$, the connecting rod with its center of mass being $S_2(x_2, y_2)$, the crosshead with its center of mass being $S_3(x_3, y_3)$, and the piston rod which has force (F_h) on crosshead in the horizontal direction if there is no the crosshead subsidence.

Brief analyses for the model are shown in Figures 2(a) and 2(b) which show two general positions of the crank. As is seen from the analysis, in any positions, the force F_{r23} on crosshead will always be vertically downward so that the crosshead will never jump if the crosshead does not subside.

From Figure 2, it is clear that if the crosshead subsidence is omitted, the crosshead will never jump from its track. However, when it comes to the model that considers the factor mentioned above, the jumping behavior for crosshead will take place. The model that takes into consideration the crosshead subsidence is shown in Figure 3. The parameter d is used to describe how much the abrasion is. Actually, the real crosshead subsidence is far less than that shown in Figure 3 to make it clearer to analyze what happened to the model when there is the crosshead subsidence. There are four critical positions named 1, 2, 3, and 4 in every revolution of the crank.

According to different force situations in Figure 3, four charts of dynamic analysis for different positions of the crank are shown in Figure 4. It is obvious that during the position 1-2 and 3-4, the direction of force F_{r23} on crosshead always has a vertical upward component that makes the crosshead jump from its track. However, during position 2-3 and 4-1, the direction of force F_{r23} on crosshead always has a vertical downward component that makes the crosshead contact the track closely. Simply speaking, if the gravity of the connecting rod and crosshead and the deformation force of piston rod on crosshead are omitted, the crosshead will jump during position 1-2 and 3-4. In the next several section, many factors including the gravity of connecting rod, the gravity of crosshead, the deformation force of piston rod on crosshead, and a small fluctuation of crank's speed are taken into consideration to simulate the real work situation.

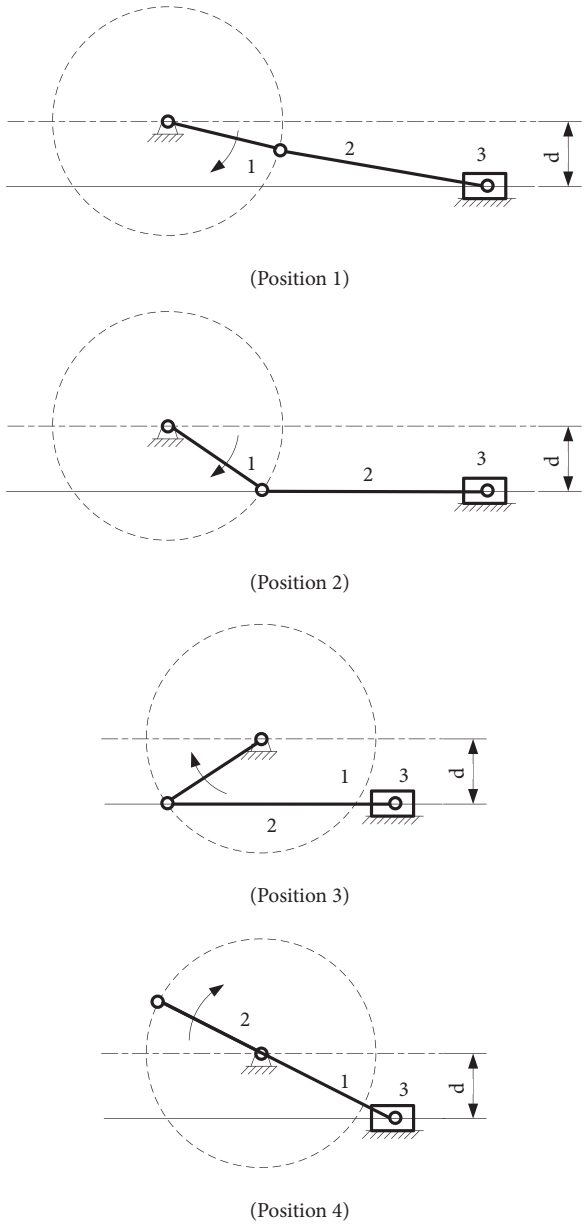

Figure 3: Four critical positions of F_{r23} for the exaggerated model.

3. Mechanical Model of Piston Rod considering the Crosshead Subsidence

As is shown in Figure 5, the model for a reciprocating compressor is simplified as composed of 4 components. Component 1 is the crank shaft with its center of mass being $S_1(x_1, y_1)$. Component 2 is the connecting rod with its center of mass being $S_2(x_2, y_2)$. Component 3 is the crosshead with its center of mass being $S_3(x_3, y_3)$. Component 4 is the piston rod which has force on crosshead both in horizontal and vertical direction. d denotes the value of how much the crosshead deviates from the original level because of the crosshead subsidence. The length of crank is r and the length of connecting rod is l. The ground is marked as component 5 which is static all the time. θ is the angle of crank (the positive direction is clockwise), and φ is the angle between connecting rod and the horizontal line. M is the driving torque on the crank. F_{r51x} and F_{r51y} are horizontal and vertical forces on the joint of the crank. F_{r53x} is the friction force on the crosshead and F_{r54} is the force which makes the piston rod in the shape shown in Figure 6. F_n which can be known as the contact force between crosshead and its track is the force acted on the crosshead by the ground. Because of the crosshead subsidence d between crosshead and its track, the piston rod was bended as shown in Figure 6 which is the detailed views of the piston rod in Figure 5.

For piston rod, there are two forces: F_v' which is the interaction force of F_v and is acted on the piston rod and F_h which is from the air cylinder. F_v, which will be introduced in the following passage, is the force acted on the crosshead. The crank will rotate in the clockwise direction, and the positive direction for the angle of crank is also set to be clockwise.

Firstly, the law of F_v' will be studied according to Figure 6. Equations (1)-(8) are the deduction of the vertical force F_v'. During the whole deduction, the piston rod is considered as a cantilever beam whose length is varied according to the length L shown in Figure 6, which is quite different from a general cantilever beam. What is more, another difference is that the place on which the vertical force acted is always at the end of the piston rod, rather than a removable force. But during the analysis process, a removable force P is considered at the position (x, y) to make it easier to deduce the equation. When the relationship between P and y is deduced, the relationship between F_v' and y can be calculated. The integral method is utilized twice to solve the differential equation.

Approximate equation of deflection curve is given in (1). After omitting the high order infinitesimals in (2), a more brief equation is shown in (3).

$$\frac{1}{\rho(x)} = \frac{M(x)}{EI_z} \tag{1}$$

$$\frac{1}{\rho(x)} = \frac{\left|y''(x)\right|}{\sqrt[2]{\left[1 + (y')^2\right]^3}} \tag{2}$$

$$\frac{d^2y}{dx^2} = -\frac{M(x)}{EI_z} \tag{3}$$

where EI_z means the bending resistance of the material of piston rod, $M(x)$ denotes the bending moment on the cross section, and the reciprocal of $\rho(x)$ denotes the curvature at the position x. The deflection equation after integration twice is given in

$$EI_z y = -\int \left[\int M(x)\,dx\right] dx + C_0 x + D_0 \tag{4}$$

where C_0 and D_0 are related to the initial conditions of a beam shown in (5). After substituting the initial condition to the equation, giving the value of d to y, and making x equal to L, the P in (5) is actually the value of F_v' which is the force at the left termination of the piston rod given in (8). To make the coordinate in this section consistent with the coordinate

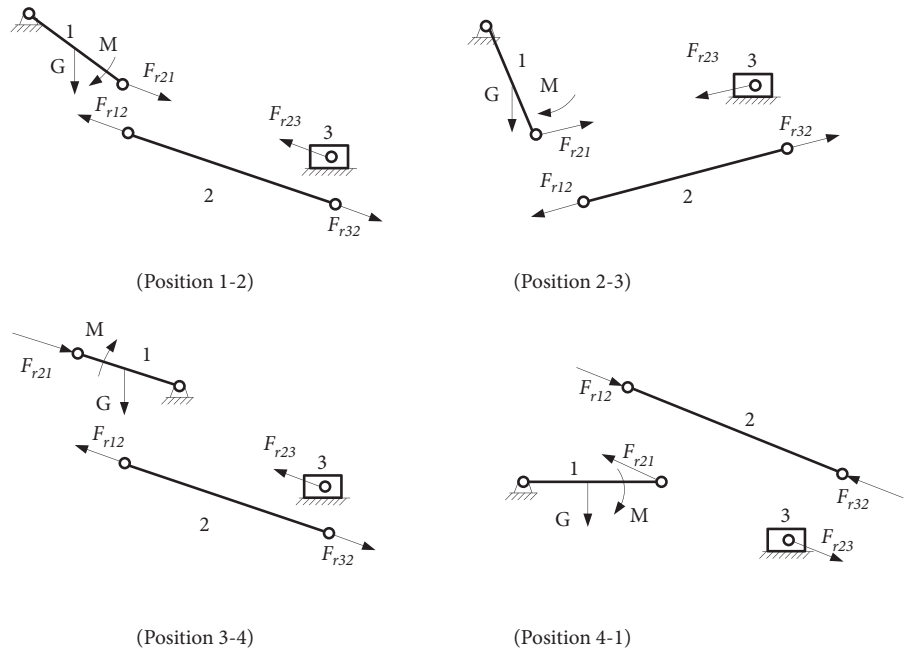

Figure 4: Brief force analysis of the model considering exaggerated crosshead subsidence in four periods.

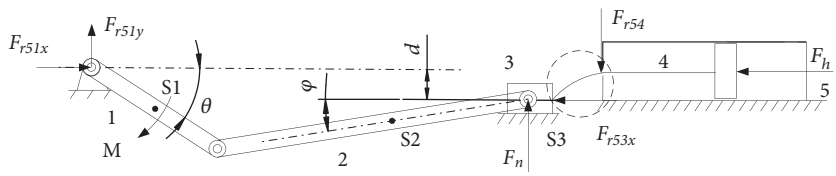

Figure 5: Schematic of reciprocating compressor considering exaggerated crosshead subsidence.

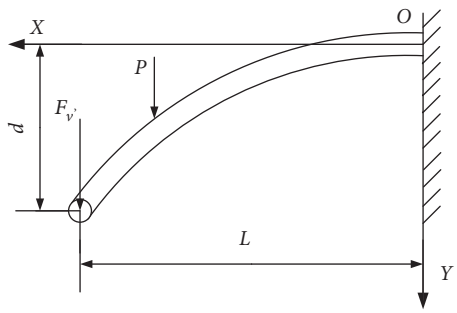

Figure 6: Detailed view of piston rod circled in Figure 5.

in Figures 5 and 6, another substitution is conducted in (9) where x_3 is the displacement of the crosshead.

$$EI_z y = \frac{P}{6}(L - x)^3 + C_0 x + D_0 \tag{5}$$

$$\begin{aligned} y(0) &= 0, \\ y'(0) &= 0 \end{aligned} \tag{6}$$

$$\begin{aligned} y &= d, \\ x &= L, \\ P &= F_v \end{aligned} \tag{7}$$

$$F_v = \frac{3dEI_z}{L^3} \tag{8}$$

$$L = S_0 + r + l - x_3 \tag{9}$$

L, S_0, and x_3 denote the length of the piston rod that bears the deformation, the length of the clearance space, and the displacement of crosshead with θ being the independent variable, respectively. Details of L in (8) are given in (9). S_0 is an important parameter for different reciprocating compressors. The adoption of parameter S_0 has large influences on the force. However, for a specific reciprocating compressor, values of these parameters are given in advance so that we do not have to study the changing law of parameter S_0. Parameters for the 2D12 compressor will be given in Table 1 so that the value of the forces can be calculated. To simplify the model, the second stage of the cylinder was omitted so that we can focus the attention on the dynamic response of crosshead.

To conclude, the numerical solution of F_v can be given on condition that the data of x_3 has already been solved according to the specific motion. Curves of F_v-x_3 and curve of F_v-θ are shown in Figures 7(a) and 7(b) on condition that the value of crosshead subsidence d is 1mm. Additionally, the value of d can be changed according to the size of crosshead subsidence.

Table 1: Parameters of 2D12 reciprocating compressor.

m_1/kg	m_2/kg	m_3/kg	r/m	l/m	E/Gpa
1	5	1	0.120	0.600	207

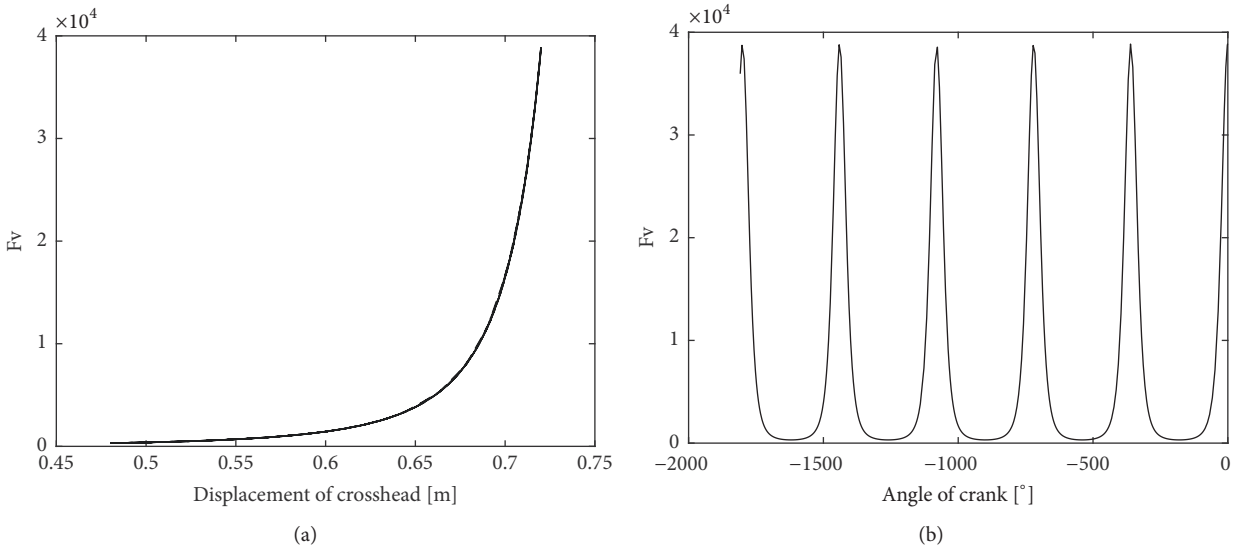

Figure 7: Deformation force on crosshead (F_v) with different x-coordinates.

Secondly, F_h is the horizontal force acted by the piston rod which is originally caused by the change of gas pressure in the air cylinder. F_h can be derived by assuming that the expansion and compression process is isentropic and air is of ideal gas. The force of friction between the crosshead and the track is not too significant to be counted in, compared with F_h. The equation for the cylinder pressure F_h of each stage can be derived from the law of thermodynamics given in

$$F_h = \begin{cases} P_{out}\left(\dfrac{S_0}{S_0 + r + l - x3}\right)^m & Expansion \\ P_{in} & Suction \\ P_{in}\left(\dfrac{S + S_0}{S_0 + r + l - x3}\right)^m & Compression \\ P_{out} & Exhaust \end{cases} \tag{10}$$

where P_{in} and P_{out} are the inlet and discharge pressure, respectively. S and S_0 are the piston stroke and piston clearance, respectively. x_3 is the displacement of crosshead, and m is the expansion exponent which is usually 1.14 for medium and large scale reciprocating compressors according to thermal dynamic analysis. The relationship between F_h and the displacement of crosshead is given in Figure 8.

4. Equations of the Model for Reciprocating Compressors considering Crosshead Subsidence

First of all, some geometric relationships will be shown to do some previous work for equations of motion, as shown in Figure 5.

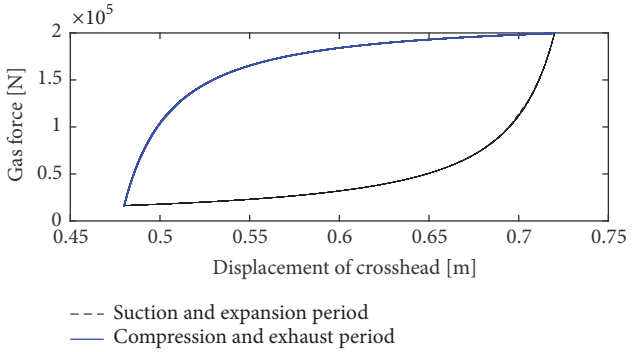

Figure 8: Gas force acted on the piston rod.

Positions of the three parts' mass center are given in (11)-(13), respectively:

$$x_1 = \frac{1}{2} r \cos\theta, \qquad y_1 = \frac{1}{2} r \sin\theta \tag{11}$$

$$x_2 = r\cos\theta + \frac{1}{2} l \cos\varphi, \qquad y_2 = r\sin\theta - \frac{1}{2} l \sin\varphi \tag{12}$$

$$x_3 = r\cos\theta + l\cos\varphi, \qquad y_3 = -d = r\sin\theta - l\sin\varphi \tag{13}$$

where r is the length of crank and l is the length of connecting rod. The piston rod is considered to be connected with the crosshead, so displacement of the piston rod is ignored in this paper. The velocity and acceleration of each mass center can be derived from the above equations by calculating their first and second derivative. The constraint condition of the system is given in (14).

$$r \sin \theta + d = l \sin \varphi \tag{14}$$

With (14), the whole function can be transformed to a one-degree freedom. In this section, equations of motion for a reciprocating compressor are shown in (15), taking into consideration the mass of both the crank and the connecting rod that would otherwise be ignored by many other papers. What is more, the vertical force generated by the deformation of piston rod is also considered since the force has the same magnitude as the horizontal force generated by the piston rod. The Lagrange equation of motion is given as

$$\frac{d}{dt}\left(\frac{\partial L}{\partial \dot{q}_j}\right) - \frac{\partial L}{\partial q_j} = \mathscr{F} \tag{15}$$

where L equals T minus V. T and V are the kinetic and potential energy of each part, respectively. The specific forms of T and V are shown in

$$T = T_1 + T_2 + T_3 \tag{16}$$

$$T_1 = \frac{1}{2} I_1 \dot{\theta} = \frac{1}{2}\left(\frac{1}{3} m_1 r^2\right)\dot{\theta}^2 = \frac{1}{6} m_1 r^2 \dot{\theta}^2 \tag{17}$$

$$\mathrm{T}_2 = \frac{1}{2}\mathrm{I}_2 \dot{\varphi}^2 + \frac{1}{2}\mathrm{m}_2 \dot{\mathrm{x}}_2^2 + \frac{1}{2}\mathrm{m}_2 \dot{\mathrm{y}}_2^2 \tag{18}$$

$$T_3 = \frac{1}{2} m_3 \dot{x}_3^2 \tag{19}$$

$$V = V_1 + V_2 + V_3 \tag{20}$$

$$V_1 = m_1 g y_1 = \frac{1}{2} m_1 g l \sin \theta \tag{21}$$

$$V_2 = m_2 g y_2 = m_2 g \left(r \sin \theta - \frac{1}{2} l \sin \varphi\right) \tag{22}$$

$$V_3 = -m_3 g d \tag{23}$$

where T_1, T_2, and T_3 represent the kinetic energy of the crank, linkage, and slider, respectively. V_1, V_2, and V_3 denote the potential energy of gravity with the surface over the center of crosshead being the zero potential surface. 'd' in (23) is applied to describe how much the crosshead subsidence is. $\mathscr{F}$ in (15) denotes the general force associated with the general coordinates θ in this model. In this paper, there is only a degree of freedom. The concrete form of $\mathscr{F}$ is given as

$$\mathscr{F} = M d\theta - F_h dx_3 \tag{24}$$

where M is the driving torque of the system and dx_3 is the first derivative of x_3 which is the displacement of crosshead. If the value of $\mathscr{F}$ is 0, this system is classified as conservative system in which the mechanical energy keeps unchanged. From the formation of (24), $\mathscr{F}$ is composed of two components: the virtual work of driving torque and resistance. Suppose that the speed of the crank is in a rather stable speed around a certain value, virtual work $\mathscr{F}$ should be a changing parameter around 0 so that the system can be in a stable situation. Before this paper, almost every scholar focuses their attention on the model of reciprocating compressor without considering the crosshead subsidence. Also, they usually assume that the rotation speed is a constant number under a certain kind of running condition in a conservative system also known as the system in which the mechanical energy is conservative. In this paper, there is a slight difference in the adoption of $\mathscr{F}$ to simulate a model that is more close to the real running situation. Based on D'alembert's principle, F_h can be classified as the constraint force, which means the impact of the force does not have to be ignored during the whole modeling of Lagrange's equation. However, for this ignorance there is a precondition that the crosshead should not have any displacement in the vertical direction. In this work, the value of d is given a series number to analyze the difference that the parameter d will make. Although there are vibrations in the vertical direction, the virtual work made by the crosshead is too little to have some influence on the system.

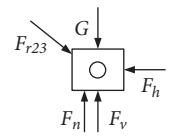

Figure 9: Mechanical analysis on crosshead.

As a consequence, Lagrange's equation can be built up without considering the virtual work of the F_v which is the vertical force generated by the deformation of piston rod. Substituting values in Table 1 into (15), we get the final equation as given in

$$F_1(\theta) \times \ddot{\theta} + F_2(\theta) \times \dot{\theta}^2 = F_3(\theta) \tag{25}$$

where $F_1(\theta)$, $F_2(\theta)$, $F_3(\theta)$ represent functions of θ. Due to the complexity of the three functions, details are not given here. The purpose of taking the three functions was only to get a more concise form of the final kinetic function. Finally, the numerical solutions can be obtained through ODE, which is a very useful tool to solve differential equations.

In the Lagrange's equation, the vertical force F_v on crosshead generated by the deformation of the piston rod is considered as a constraint force and its virtual work is zero so that it can be neglected to simplify the model. Nevertheless, the constraint force does exist and has great influences on the behaviors of crosshead. When the Lagrange's equation is solved, any dynamic data of every parts of the system are all available through this solver. And then combining the responses with the constraint force F_v, some hidden vibration in the vertical direction appears.

To fully illustrate the process, the arithmetic process will be introduced in detail in Figure 9.

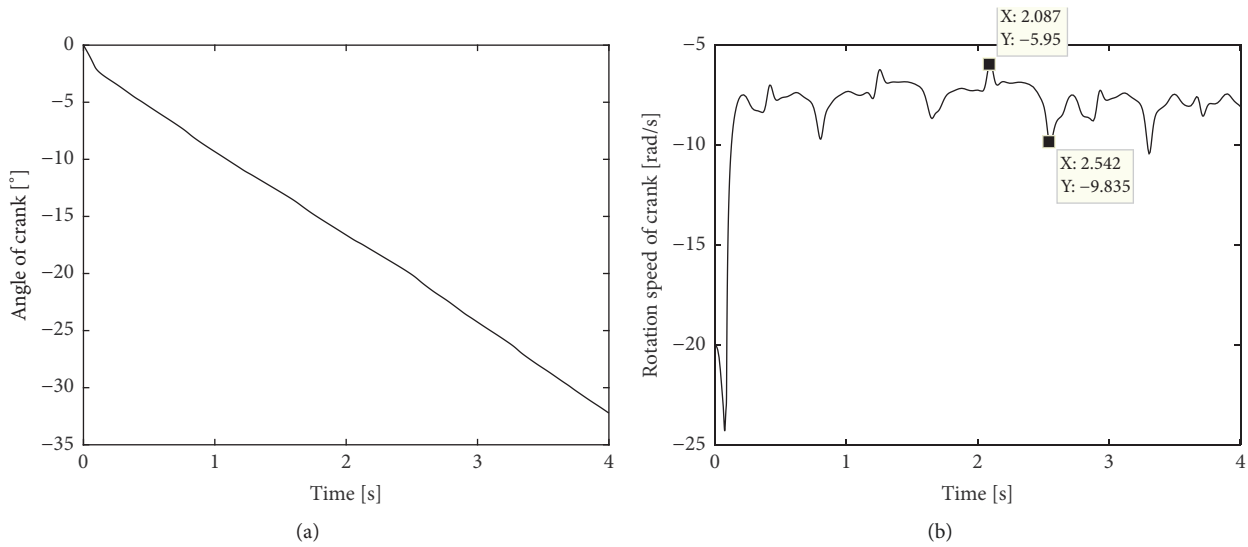

Figure 10: Crank rotation angle and crank rotation speed.

Because of the uncertainty of the force F_v, we assume that the deformation is always at its maximum (actually, most of the time, the crosshead contacts the track closely). Once the value of F_v is bigger than the vertical component of F_{r23}, the crosshead will jump to its original level. To make it easier to understand, F_n is introduced to represent the contact force between crosshead and its track. We assume that the crosshead always contacts the track closely. According to this assumption, the value of F_n should always be positive. Once the value turns to zero or negative, it means the crosshead has already jumped from its track.

According to Newton's second law, horizontal analysis for crosshead is given in

$$m_3\ddot{x}_3 = F_{r23}\cos\varphi - F_h - F_{r53x} \tag{26}$$

where m_3 is the mass of crosshead and $\ddot{x}_3$ is the acceleration of crosshead. Compared with F_{r23} and F_h, the value of F_{r53x} is several thousand times less so it can be omitted to simplify the model. F_{r23} can be calculated through (26) and the total force imposed on the crosshead in the vertical direction is calculated in

$$F_n = F_{r23}\sin\varphi - F_v + G \tag{27}$$

where F_n is the contact force between crosshead and its track. Once the value of F_n turns to negative, it means F_v no longer exists and the crosshead will jump from its track which is the source of vibration.

5. Results and Analysis of the Model considering Crosshead Subsidence

The initial rotation speed of crank was set to be around 20rad/s but a fluctuation is added to simulate the real working situation of the motor. Initial value of (26) is [0,-20], which is calculated by ODE15S in MATLAB. The numerical results are crank rotation angle and crank rotation speed, as shown in Figures 11(a) and 11(b).

From Figure 10(a), it can be seen that except for the speed near 0 seconds, the crank rotation angle and time basically maintain a linear relationship, and the speed value is negative. It also rotates in the expected direction. Considering the virtual work done by external forces, the crank simulation is successful. From Figure 10(b), it can be seen that the crank's speed fluctuates basically at a certain value in other time periods besides the large fluctuation of its velocity near zero value. The figure includes the start-up stage and normal operation stage. When the crank is in normal operation stage, because of the superposition of positive and negative work, the speed will fluctuate slightly. The positive work of the system comes from the motor driving the crank to rotate, and the negative work comes from the negative work of the external force at the piston end.

Three cases are shown to fully illustrate the dynamic responses of crosshead and the messages it carries. The values of crosshead subsidence are 0.1mm, 0.4mm, and 0.7mm, respectively.

Figure 11 shows $F_{r23} \bullet \sin\varphi$ and F_v in the three given cases with the angle of crank being the x-coordinate. As can be easily seen in Figure 11, forces exerted on the crosshead in the vertical direction have two main sources, $F_{r23} \bullet \sin\varphi$ (the vertical component of F_{r23}) and F_v. The gravity of the crosshead is too tiny to make some difference so that it is omitted. To conclude, where there are intersections in Figure 11, the crosshead will jump. With the increase of crosshead sinking, the force of connecting rod and piston rod against crosshead is closer and closer; that is to say, the larger the sinking, the greater the possibility of jumping and the stronger the vibration.

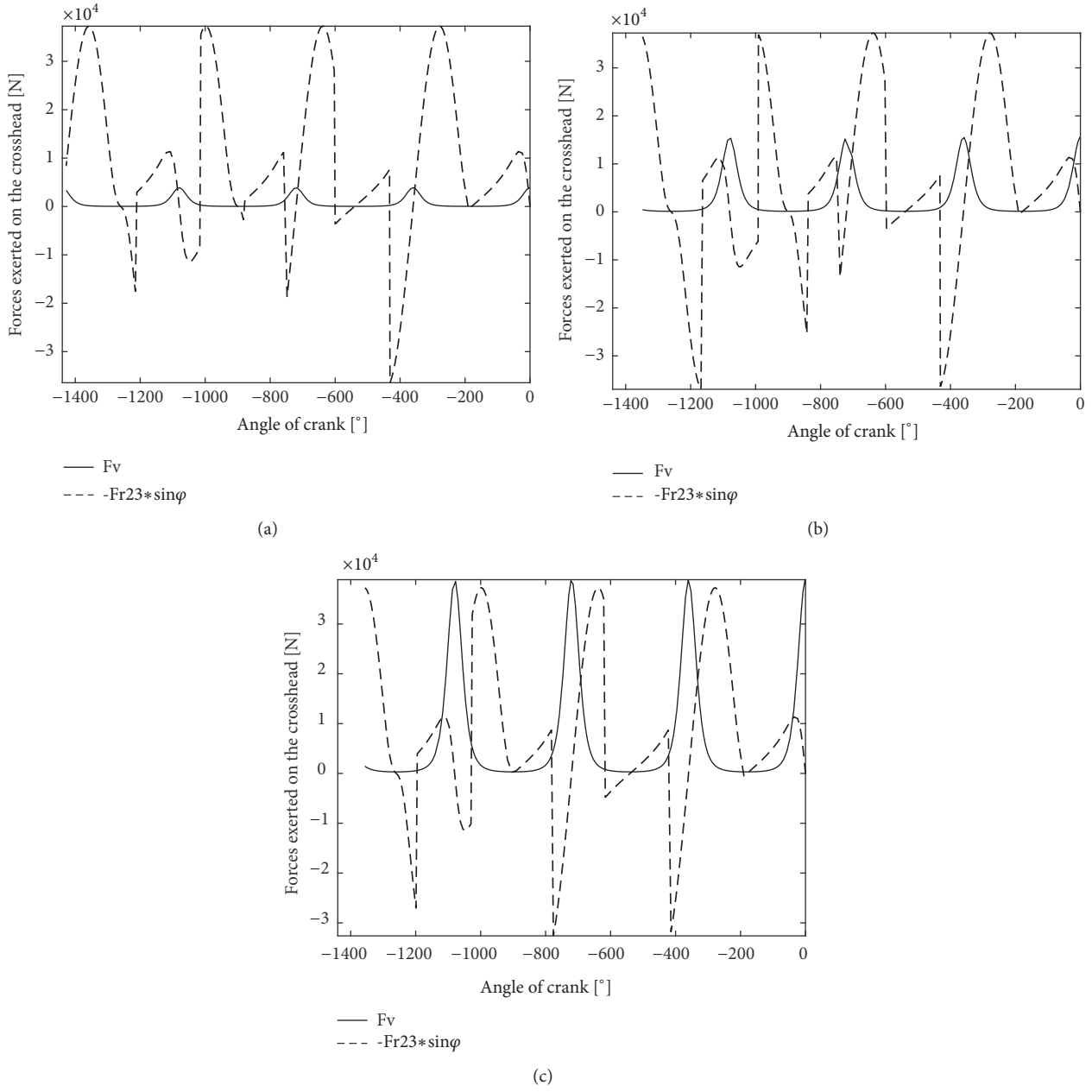

Figure 11: Forces of $F_{23} \sin \varphi$ and F_v.

To make it easier to understand, the difference values of the two forces are shown in Figure 12, which can be known as the contact force (F_n) between the track and the crosshead supposing that the crosshead contacts the track all the time. In Figure 12, where there are intersections between the curve and the zero line, there are vertical vibrations. Figures 12(a), 12(b), and 12(c) are simulations on condition that the crosshead subsidence values are 0.1mm, 0.4mm, and 0.7mm, respectively.

To make Figures 11 and 12 clearer, the first period of the motion was taken as a sample which is shown in Figure 13. It is clear that the value of contact force F_n between two objects should always be positive supposing that two objects always contact each other all the time. Under this assumption, if the negative value in Figure 12 appears, this means that the crosshead and the track are separated from each other. It is clear from the curve in Figure 13 that there are four intersections with the zero line but with different crosshead subsidence d. Figures 13(a), 13(b), and 13(c) are the contact force with the crosshead subsidence being 0.1mm, 0.4mm, and 0.7mm, respectively.

Figure 14(a) puts the three curves of contact force in Figure 13 in the same figure so that some conclusions can be drawn. Figure 14(b) is the detailed view around angle 180° in Figure 14(a).

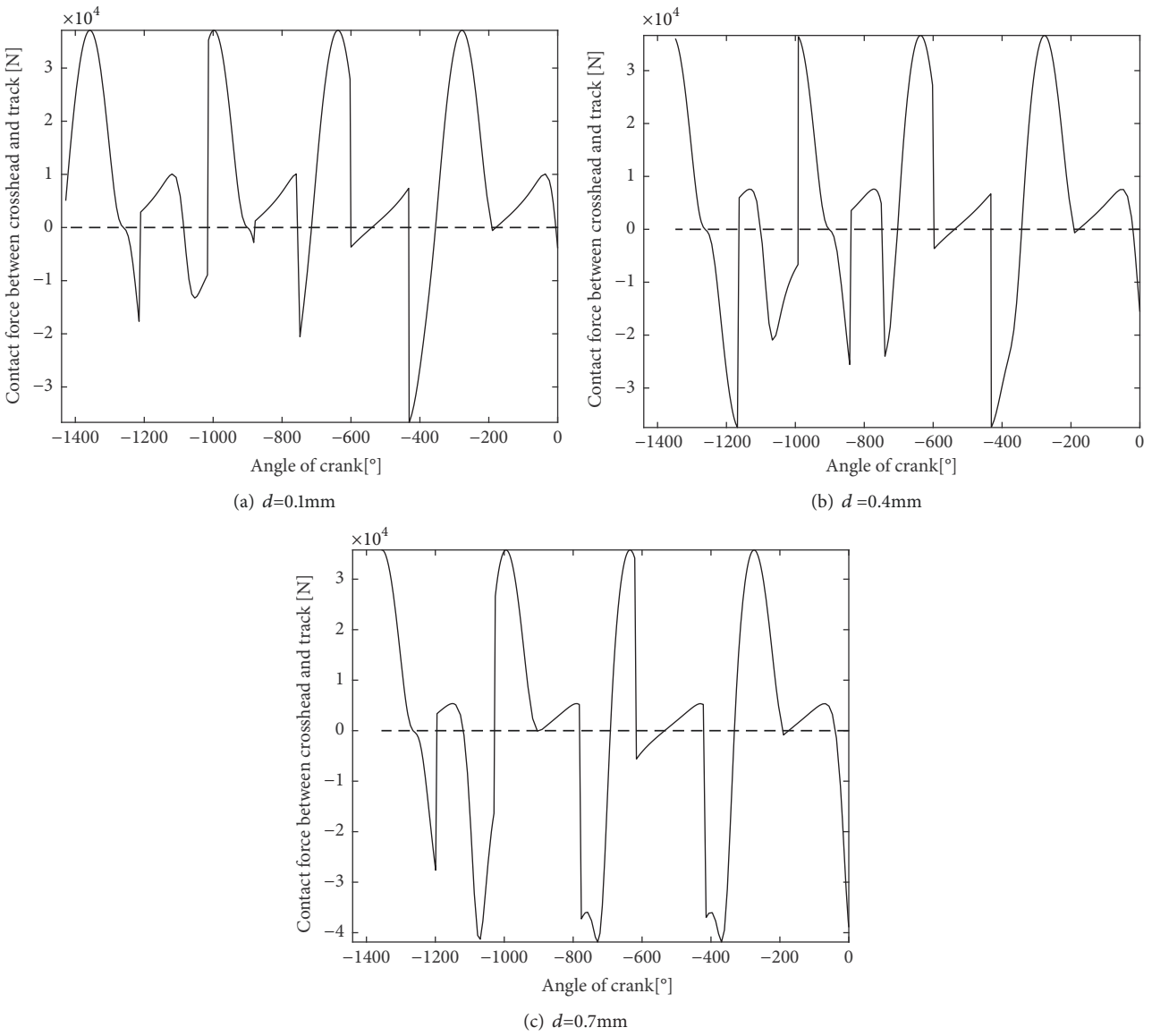

Figure 12: The contact force between crosshead and its track.

It can be seen from Figure 14 that there are four intersection points in different locations, because the amount of subsidence is different. The earliest jump occurs when d =0.1mm because the amount of subsidence is relatively small, which is consistent with the actual working conditions. The last jump takes place when d =0.7mm, because the amount of subsidence is relatively large. Detailed view of the curves in a working period is given in Figure 14(b).

As can be seen from the figure, the order of the second jump is when d = 0.1mm, d = 0.4mm, and d = 0.7mm, respectively. The order of the third jump is the same as that of the first jump.

With the variation of the crosshead subsidence, the position where the jumps take place also varies. There is certain regularity between the order of jump and the amount of crosshead subsidence.

6. Conclusions

In order to analyze the vibration mechanism in a reciprocating compressor with crosshead subsidence between crosshead and track, a model based on Lagrange equation considering the flexibility of the piston rod is built in a rather stable running situation.

To conclude, if the flexibility of the piston rod is considered, extra vibration especially in the vertical direction will undoubtedly take place. During a working period, the times of the impact caused by the crosshead will be varied according to how much crosshead subsidence exists. In this paper, for the first time, the crank angle is taken as the generalized coordinate, and the crank is of variable speed. The velocity curve can simulate the start-up and normal working stages of

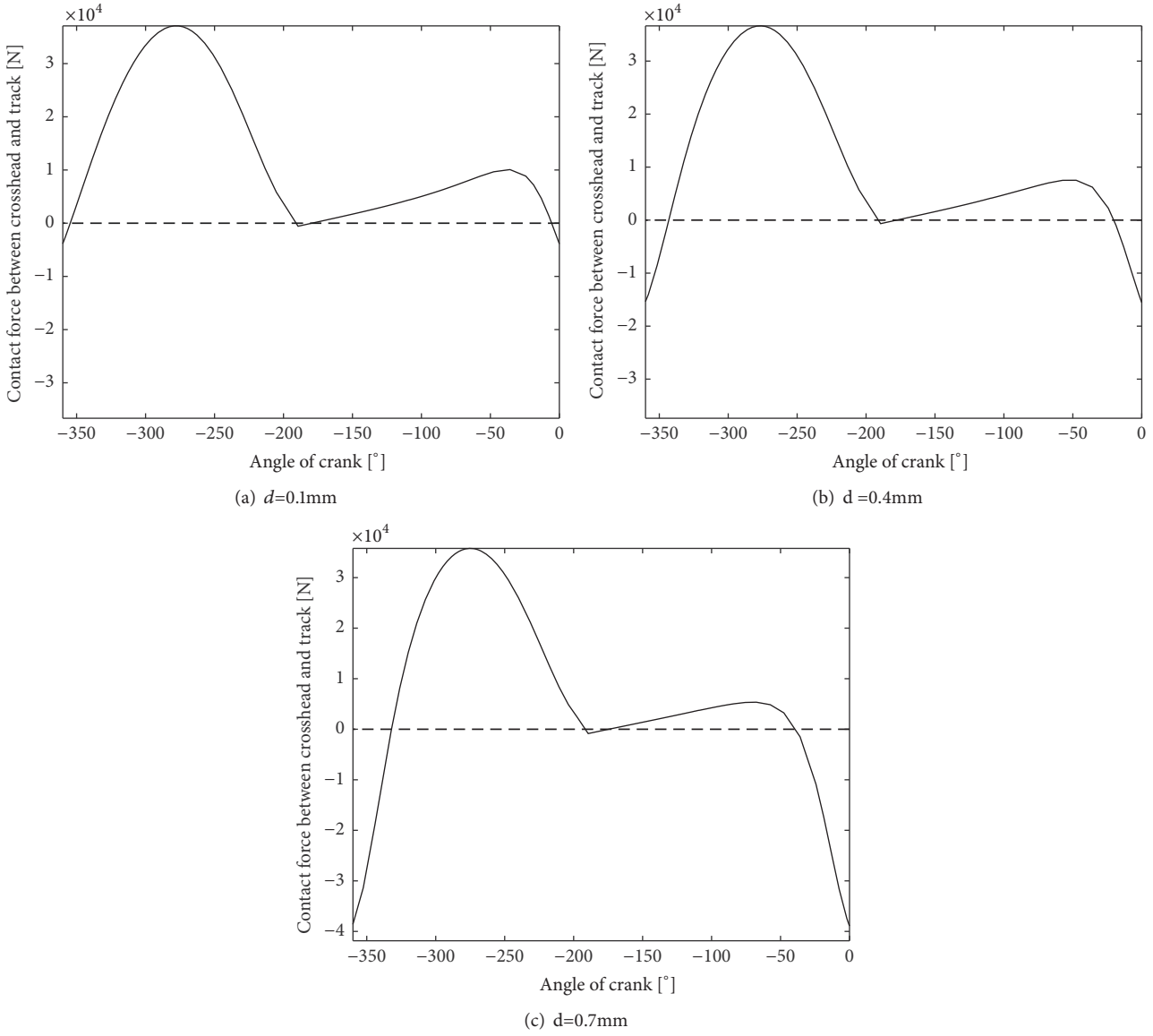

Figure 13: Contact force between crosshead and its track.

the reciprocating compressor. The influence of the flexibility of the piston rod on the sinking failure of the reciprocating compressor is also considered. It lays a good foundation for dynamic modeling of reciprocating compressor under real working conditions, which provide reference for fault diagnosis and signal processing of reciprocating compressor. It is of far-reaching significance to further study the failure of the valve of the reciprocating compressor, the vibration of the pipeline, the flexible action of the mechanism components, and the clearance collision model and to establish a more realistic mathematical model.

For every reciprocating compressor, the Lagrange model can be built only with different parameters. The result in this paper can also explain why the abrasion between crosshead and it track becomes more serious as time goes by. These impacts will aggregate the abrasion, and if the crosshead subsidence is getting more and more serious, the impacts will undoubtedly get more series. This is the reason why regular replacement of components is indispensable.

Data Availability

The data used to support the findings of this study are included within the article.

Conflicts of Interest

The authors declare that there are no conflicts of interest regarding the publication of this paper.

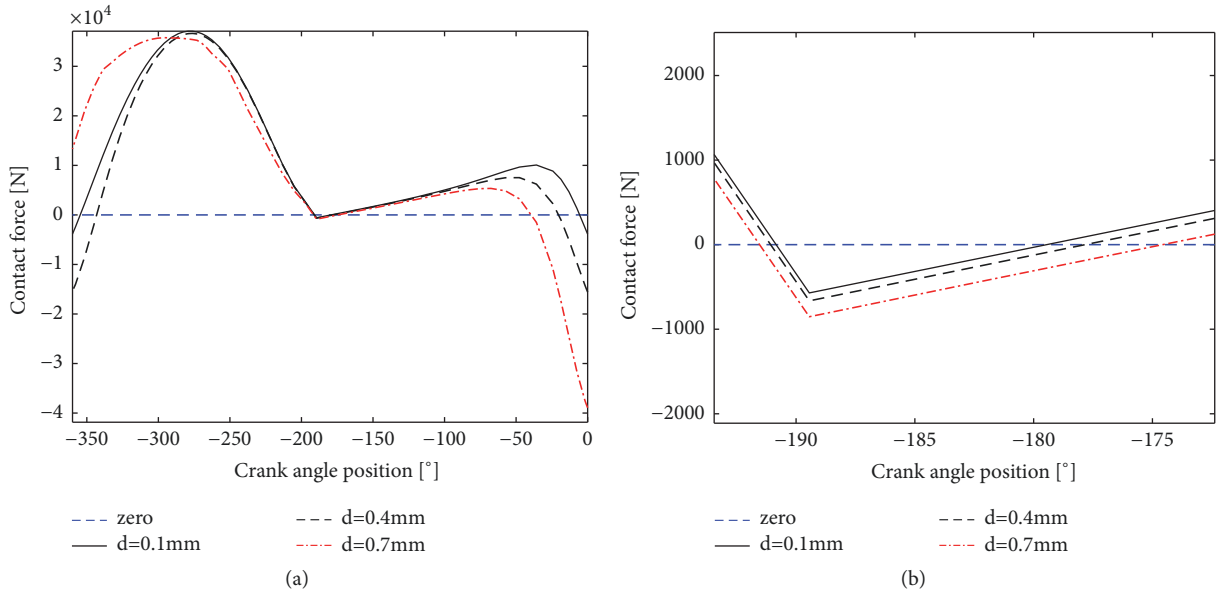

Figure 14: Comparison of the three curves.

Acknowledgments

This work is supported by the Natural Science Foundation of China (51575331), Natural Science Foundation of the Jiangsu Higher Education Institutions of China (Grant No. 16KJB460001), Science-Technology Support Plan of Changzhou City (Grant No. CE20175044), Research Project for Yong and Middle-Aged Teachers in Fujian Province (Grant No. JT180601), and Young Teacher Special Project of Ningde Normal University (Grant No. 2018Q101).

References

[1] A. Almasi, "A new study and model for the mechanism of process reciprocating compressors and pumps," *Proceedings of the Institution of Mechanical Engineers, Part E: Journal of Process Mechanical Engineering*, vol. 224, no. 2, pp. 143–147, 2010.

[2] Z. Hai-Yang, X. Min-Qiang, W. Jin-Dong, and L. Yong-Bo, "A parameters optimization method for planar joint clearance model and its application for dynamics simulation of reciprocating compressor," *Journal of Sound and Vibration*, vol. 344, pp. 416–433, 2015.

[3] V. Parlaktaş and E. Tanik, "Single piece compliant spatial slider-crank mechanism," *Mechanism and Machine Theory*, vol. 81, pp. 1–10, 2014.

[4] J. F. Deck and S. Dubowsky, "On the limitations of predictions of the dynamic response of machines with clearance connections," *Journal of Mechanical Design*, vol. 116, no. 3, pp. 833–841, 1994.

[5] D. Ndiaye and M. Bernier, "Dynamic model of a hermetic reciprocating compressor in on-off cycling operation (Abbreviation: Compressor dynamic model)," *Applied Thermal Engineering*, vol. 30, no. 8-9, pp. 792–799, 2010.

[6] M. Farzaneh-Gord, H. R. Rahbari, M. Bajelan, and L. Pilehvari, "Investigation of hydrate formation in natural gas flow through underground transmission pipeline," *Journal of Natural Gas Science and Engineering*, vol. 15, pp. 27–37, 2013.

[7] R. Singh and W. Soedel, "Mathematical modeling of multicylinder compressor discharge system interactions," *Journal of Sound and Vibration*, vol. 63, no. 1, pp. 125–143, 1979.

[8] M. Farzaneh-Gord and H. Khoshnazar, "Valve fault detection for single-stage reciprocating compressors," *Journal of Natural Gas Science and Engineering*, vol. 35, pp. 1239–1248, 2016.

[9] V. T. Tran, F. Althobiani, and A. Ball, "An approach to fault diagnosis of reciprocating compressor valves using Teager–Kaiser energy operator and deep belief networks," *Expert Systems with Applications*, vol. 41, no. 9, pp. 4113–4122, 2014.

[10] K. Brun, S. Simons, and R. Kurz, "The impact of reciprocating compressor pulsations on the surge margin of centrifugal compressors," in *Proceedings of the ASME Turbo Expo 2016: Turbomachinery Technical Conference and Exposition*, pp. 13–17, Seoul, South Korea, 2016.

[11] P. Flores, "A parametric study on the dynamic response of planar multibody systems with multiple clearance joints," *Nonlinear Dynamics*, vol. 61, no. 4, pp. 633–653, 2010.

[12] P. Flores, R. Leine, and C. Glocker, "Modeling and analysis of planar rigid multibody systems with translational clearance joints based on the non-smooth dynamics approach," *Multibody System Dynamics*, vol. 23, no. 2, pp. 165–190, 2010.

[13] P. Flores and J. Ambrósio, "On the contact detection for contact-impact analysis in multibody systems," *Multibody System Dynamics*, vol. 24, no. 1, pp. 103–122, 2010.

[14] X. Jia, D. Jin, L. Ji, and J. Zhang, "Investigation on the dynamic performance of the tripod-ball sliding joint with clearance in a crank-slider mechanism. Part 1. Theoretical and experimental results," *Journal of Sound and Vibration*, vol. 252, no. 5, pp. 919–933, 2002.

[15] S. Yaqubi, M. Dardel, and H. M. Daniali, "Nonlinear dynamics and control of crank-slider mechanism with link flexibility and joint clearance," *Proceedings of the Institution of Mechanical Engineers, Part C: Journal of Mechanical Engineering Science*, vol. 230, no. 5, pp. 737–755, 2016.

[16] I. Khemili and L. Romdhane, "Dynamic analysis of a flexible slider-crank mechanism with clearance," *European Journal of Mechanics - A/Solids*, vol. 27, no. 5, pp. 882–898, 2008.

[17] A. L. Schwab, J. P. Meijaard, and P. Meijers, "A comparison of revolute joint clearance models in the dynamic analysis of rigid and elastic mechanical systems," *Mechanism and Machine Theory*, vol. 37, no. 9, pp. 895–913, 2002.

[18] Z. Wang, Q. Tian, H. Hu, and P. Flores, "Nonlinear dynamics and chaotic control of a flexible multibody system with uncertain joint clearance," *Nonlinear Dynamics*, vol. 86, no. 3, pp. 1571–1597, 2016.

[19] M. Dupac and D. G. Beale, "Dynamic analysis of a flexible linkage mechanism with cracks and clearance," *Mechanism and Machine Theory*, vol. 45, no. 12, pp. 1909–1923, 2010.

[20] S. Erkaya and I. Uzmay, "Effects of balancing and link flexibility on dynamics of a planar mechanism having joint clearance," *Scientia Iranica*, vol. 19, no. 3, pp. 895–913, 2012.

[21] S. Erkaya, S. Doğan, and E. Şefkatlıoğlu, "Analysis of the joint clearance effects on a compliant spatial mechanism," *Mechanism and Machine Theory*, vol. 19, no. 3, pp. 895–913, 2016.

[22] Q. Tian, Y. Zhang, L. Chen, and J. Yang, "Simulation of planar flexible multibody systems with clearance and lubricated revolute joints," *Nonlinear Dynamics*, vol. 60, no. 4, pp. 489–511, 2010.

[23] S. Erkaya and I. Uzmay, "Modeling and simulation of joint clearance effects on mechanisms having rigid and flexible links," *Journal of Mechanical Science and Technology*, vol. 28, no. 8, pp. 2979–2986, 2014.

[24] S. Erkaya, "Clearance-induced vibration responses of mechanical systems: computational and experimental investigations," *Journal of the Brazilian Society of Mechanical Sciences and Engineering*, vol. 40, no. 2, p. 90, 2018.

[25] S. Erkaya, "Experimental investigation of flexible connection and clearance joint effects on the vibration responses of mechanisms," *Mechanism and Machine Theory*, vol. 121, pp. 515–529, 2018.

[26] E. Zheng and X. Zhou, "Modeling and simulation of flexible slider-crank mechanism with clearance for a closed high speed press system," *Mechanism and Machine Theory*, vol. 74, pp. 10–30, 2014.

[27] S. Xiao, S. Liu, S. Cheng, X. Xue, M. Song, and X. Sun, "Dynamic analysis of reciprocating compressor with clearance and subsidence," *Journal of Vibroengineering*, vol. 19, no. 7, pp. 5061–5085, 2017.

[28] S. Xiao, H. Zhang, S. Liu, F. Jiang, and M. Song, "Dynamic behavior analysis of reciprocating compressor with subsidence fault considering flexible piston rod," *Journal of Mechanical Science and Technology*, vol. 32, no. 9, pp. 4103–4124, 2018.